

# Computer aided detection of microcalcification clusters in mammogram images with machine learning approach

İSMAIL İŞERİ\*, CEMİL ÖZ<sup>a</sup>

*Sakarya University, Faculty of Computer and Information Sciences, Department of Computer Engineering, Esentepe Campus, Sakarya, Turkey*

<sup>a</sup>*Sakarya University, Faculty of Computer and Information Sciences, Department of Computer Engineering, Esentepe Campus, Sakarya, Turkey*

---

Breast cancer is one of the most deadly disease for women health. One of the most used method is digital mammography in medical diagnosis for breast cancer. Mammogram images are important for detecting breast cancer in early stages. Scientists works on computer aided detection systems for developing second reader systems for radiologists and for reducing detection and diagnose error rates. The complexity and difficulty of microcalcification detection is one of the initial problem in mamogram analysis. In this paper, it is proposed a new feature extraction method called multi-window based statistical analysis (MWBSA) for detection of microcalcification clusters which are early signs of breast cancer and two stage software framework as a computer aided detection and diagnosis system is proposed. The artificial neural network (ANN) is used as a classifier. Results show that multi window based approach is as applicable as other well known methods (GLCM and Wavelet) and also the computer detection system is applicable as a second reader. As a result of the ROC analysis high sensitivity values 1,00 by using MIAS database is obtained.

(Received June 11, 2014; accepted July 10, 2014)

*Keywords:* Microcalcification, Neural Networks, Classification, Detection of Breast Cancer, Mammograms, Machine Learning

---

## 1. Introduction

Breast cancer has increased significantly in recent years and continues to be an important problem that threatens the health of women all around the world. According to the latest statistics of the cancer research and cancer control unit of Turkey, breast cancer is the second most important danger of death after cardiovascular diseases. These types of cancer is at the forefront of breast cancer compared to thirty-percent. The causes of breast cancer is not known exactly yet a definite method to prevent breast cancer taken. Therefore, early detection of the disease significantly affects the rate of survival. Used in this field, mammograms, which is two-dimensional X-rays images of women chest, is playing a key role in the diagnosis of breast cancer [1,2]. The researchers are studying for early detection systems by using computerized algorithms, image processing techniques and machine learning techniques.

In the literature, a large number of computer-based application developed for the diagnosis of breast cancer are outstanding. Ertas developed in a database which stores mammographic mass shapes and also additional information such as a biopsy report in his thesis [3]. Suganthi and Madheswaran obtained the properties of texture and shape features and have made the classification of tumors using a neural network-based classifier and achieved 0.99 accuracy value in their study [4]. Tüysüz studied quick and easy identification of problematic areas on mammograms using mathematical morphology and wavelet transform providing the best picture quality

improvement stage [5]. Strickland developed a structure based on two stage wavelet transform to identify areas of microcalcification [6].

In this study, detection and classification of microcalcification clusters which are important markers for the diagnosis of breast cancer (MC) was studied. MC's seen as small white spots on mammograms are very thin accumulations of calcium. Clustered MC's are major symptoms of breast cancer. MC's appear by 30 percent or 50 percent of mammographic imaging [7]. The past two decades, the determination of the MC clusters have been studied quite extensively in the development of computer-aided systems [8-12]. A filtering approach developed by Nishikawa using the methods of image enhancement. This method intended to reduce the number of FP (False Positive) with operation of making the difference in image and the following morphological erosion operation. The difference of two image is obtained by using two filters, one of the filters presses the image while the other one is enhancing [13]. More recently, a noise equalization method is proposed by Mc Loughlin. In this study, it is assumed that the main source of noise in digital mammograms are the limited Quantized X-Ray's. The gray levels of the quantum noise is modeled using a simple square root law. The local contrast was developed by removing the noise dependence on gray level [14]. Quia developed a cluster analysis based and group-based regional approach for detection MC [15]. The similarity between these methods, the use of standard methods, before or after image processing. Gurcan at all. have used the differences between high-level statistics (volatile level

= skewness, kurtosis = fourth level) and obtained that the regions containing MC are not suitable for Gaussian distribution, the regions containing the MC are suitable for Gaussian distribution [16]. Caputo et al. developed the MRF (Markov Random Field) approach for detection of MC. This model is based on the use of "spin glass" energy functions (Generalized Gaussian Kernels) [17]. Casaseca et al. compared the Gaussian featured different methods [18]. MRF model is used by other statistical model to characterize the density distribution of an image is more advantageous. However estimation of suitable predistribution of such probabilistic approaches still remains to be complicated.

Stickland and Hahn have demonstrated MC's, with a circular Gaussian shapes of different widths in different scales using full-pulsed biorthogonal wavelet transform [19]. Later Lemaur et al. proposed that Matzinger wavelets are more suitable than classical Daubechies wavelets for the detection MC's [20]. Mini et al. were investigated multiplexed signals by assuming the mammograms are oscillation ripples [21]. Nakayama et al. combined with Bayes classifier and filter bank for the detection of MC's [22]. Regentova et al. combined with wavelet transform and hidden Markov trees maximum likelihood framework for the detection of MC's [23]. Yu and Guan developed a two stage neural network by using wavelet components, gray-level experimental statistics and shape properties [24]. The first step was for detecting potential MC's and second stage was for determining the area of each MC. Machine learning methods have the ability to share extensive research in recent years. The evolutionary methods by using genetic algorithms have been studied for MC determination of the highest and most optimal bright spots [25,26]. The biggest problem of evolutionary methods is selecting the appropriate starting point and as a result of this encountering of a numerical instability. Artificial neural networks are investigated and used in the determination of the MC's [27-30]. Together with these high nonlinearity associated with these methods can lead to encounter with the problem of the local minimum, as a result, reduce the power of discrimination. Naqa et al. used support vector classifier approach to the classification problem of MC's [31]. Singh et al. also evaluated the classification using support vector machines and they obtained 0.98 A(z) value with FROC curve. [32]. L. Wei, et al. used the structure of relevance vector machine in their study instead of SVM and obtained the same accuracy to 7.26 seconds instead of 250. This is of great importance in terms of real-time applications [33]. Rizzi et al. developed two different MC detection system using neural network and support vector machines, and have pointed to the CAD systems can be used as the second readers in radiology [34]. Peng et al. have developed a stochastic resonance based noise detection method [35]. In this study, a suitable dose of noise is added to the abnormal mammograms such that the performance of a suboptimal lesion detector is improved without altering the detector's parameters.

In our study, it is studied a two stage computer aided microcalcification detection and diagnosis system for

mammogram images. With this study, well-known and the proposed feature extraction methods applied on mammogram images containing MC's. Extracted feature vectors are separated as training and test sets and given to the multiple layer feed forwarded ANN. Receiver Operating Characteristics (ROC analysis) used for discussion and measure of the classification truth. The obtained results from the known methods and the proposed one are discussed. Also a graphical user interface is generated for the application and showing the detection and diagnosis model.

The remaining parts of the article, the materials and methods section is about the used mammographic databases (MIAS and DDSM) and used feature extraction methods. The section result and discussion is about the process of feature extraction methods and neural network classification methods and comparing the results. The section conclusion is also about the interpretation of the results and future work.

## 2. Materials and methods

*Database:* The MIAS database and DDSM databases are used in the study. The used database in this study called MIAS created by Mammographic Image Analysis Society is available free of charge [10]. Each mammogram image in the database is 1024×1024 in size and gray level format. The total number of mammogram images in the database is 322 however 119 of them are used in the experiments. This data set includes the following features: "Character of tissue background", "Class of abnormality", "Severity of abnormality", "X coordinate of center of abnormality in the image", "Y coordinate of the center of abnormality in abno image", "Approximate radius (in pixels) of a circle enclosing the abnormality."

*Feature Extraction using MWBSA:* This method is generated by referencing to the nature of microcalcification clusters. Due to MCs are higher density areas within a certain intensity groups this method is a searching operation for finding more dense pixels in a certain density. By using this method, each region of interest (ROI) is analysed by using multi window extracting statistical and probabilistic density features. The extracted features are mean, min, max, p1 and p2. p1 is windows1 sum of the pixels in window1 ( $W1$ ) in proportion to the sum of the pixels in window2 ( $W2$ ). The width between two window is called  $w_{dt}$  may be changed during the experimental to take more reliable results.

$$p1 = \frac{\sum_{i=1}^{w1} \sum_{j=1}^{w1} W1(i, j)}{\sum_{i=1}^{w2} \sum_{k=1}^{w2} W2(i, j)}$$

$W1$  and  $W2$  are the windows which have  $w1$  and  $w2$  widths and

$$p2 = \frac{\sum_{i=1}^{w1} \sum_{j=1}^{w1} W1(i, j)}{\sum_{i=1}^{w3} \sum_{k=1}^{w3} W3(i, j)}$$

W1 and W3 are the windows which have w1 and w3 widths.

Algorithm:

Step 1: Select the ROI dimension with  $m \times m$  from mammogram image

Step 2: The first window, whose window width is w1, is placed in the center of ROI and extracted the features ( $w1 < m$ )

Step 3: Second window, whose window width is w2 ( $w2 > w1$  and  $w2 < m$ ), is combined on the first one and extracted features

Step 4: The third one, whose window width is w3 ( $w3 > w2$  and  $w3 \leq m$ ), is combined to second as seen in Fig. 1 and extracted the features.

Step 5: Shift windows from left to right and go to step 1  
The feature vector of  $v$  is situated ;

$$v = [\text{mean}(W1) \text{max}(W1) \text{min}(W1) \text{mean}(W2) \text{max}(W2) \text{min}(W2) \text{mean}(W2) \text{max}(W2) \text{min}(W2) \text{p1} \text{p2}]$$

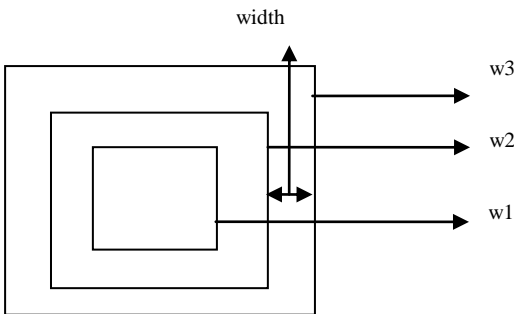


Fig. 1. Multi window based statistical analysis method and design of windows.

### 3. Results

Flow chart of the application is given in Fig. 2. The feature extraction methods applied on the 119 mammogram images in MIAS database. Totally 119 feature vector obtained. 82 of them used for training of ANN and 37 of them used for testing of ANN. Using *Gray Level Co-occurrence Matrix*:

In this study, some of the statistical properties of GLCM matrices, which are obtained from ROI areas, were extracted as feature vectors. The features included in the feature vector are 'contrast', 'homogeneity', 'energy' and 'correlation'. A feed forward multiple neuron neural network was used as a classifier. Obtained feature vectors are used for classifying the microcalcification clusters benign or malign. After the testing of neural network classifier ROC analysis was used and sensitivity value of classification is obtained as 0.81. The results for different window dimensions for searching window and different hidden neuron counts are shown in Table 1.

*Wavelet Transform*: The wavelet transform with Daubechies function is applied on the each ROI for each mammogram image four levels and horizontal, vertical and diagonal matrices direction. The matrices were used for feature extraction by calculating descriptive statistics. The descriptive statistics "mean", "median", "mode", "max", "min", "range", "std" and "mad" were included in the feature vectors. The feed forward multiple neuron neural network was used as a classifier. ROC analysis was applied on the classification results and sensitivity of 0.84 was obtained. The experimental results for different window dimensions and different hidden neuron counts are shown in Table 2.

*EWD method*: This method was applied for the first time on mammogram images in this study and sensitivity of 0.91 was obtained by using ROC analysis after classification. The feed forward multiple neuron neural network classifier used in classification stage. The flow chart of the EWD method and its algorithm are given below;

1. First of all the center coordinates of MC in mammogram image is read from a file the coordinates are written. After the ROI area is selected with 80x80 pixels (ROI choice of coordinates read from a file).

Table 1. Experimental results of GLCM method.

Window Dimension	ROC Analysis Results	Hidden Neuron Counts			
		10	20	30	40
30x30	Sensitivity (TPR)	0,88	0,75	0,88	0,75
	Fall-out(FPR)	0,62	0,48	0,66	0,45
40x40	Sensitivity (TPR)	0,75	0,75	0,96	0,88
	Fall-out(FPR)	0,69	0,76	0,90	0,72
50x50	Sensitivity (TPR)	0,81	0,70	0,89	0,74
	Fall-out(FPR)	0,69	0,52	0,69	0,34
60x60	Sensitivity (TPR)	0,75	0,75	0,88	0,88
	Fall-out(FPR)	0,48	0,62	0,83	0,59
70x70	Sensitivity (TPR)	0,74	0,70	<b>0,81</b>	0,78
	Fall-out(FPR)	0,52	0,41	0,41	0,48
80x80	Sensitivity (TPR)	0,75	0,63	0,88	0,75
	Fall-out(FPR)	0,76	0,52	0,79	0,76
<b>All Set:119</b>		<b>Training Set: 92</b>	<b>Testing Set :27</b>		

2. The window with dimension  $w = 10 \times 10$  moved from left to right direction on the ROI. The sum of the value of the pixels in the window (gray level values) is divided by the sum of the pixels of ROI. The ROI which is  $80 \times 80$  pixels is converted to a vector with dimension  $1 \times 64$ .

3. Discretization process is applied on the feature vector obtained in the previous step. Discretization parameter value K was selected as 5. For determining the optimal K value several experiments was done. In this study, the best accuracy are obtained for  $K = 5$ . The vector  $1 \times 64$  size obtained in the previous step is transformed to  $1 \times 5$  size.

4. The feature vectors with  $1 \times 5$  dimension are given to the inputs of ANN classifier. (seperating 70% of them for training and 30% for testing). 0.97 percent accuracy was obtained in the classification step. The experimental

results for EWD method is shown in Table 3. In this experiment different K values and hidden neuron counts are used and the most sensitivity value (1,00) is obtained for while K values is 64 and hidden neuron count is 20.

*Multi-window statistical analysis method:* This method is applied on the 119 mammogram images selected from MIAS mammographic database. The features calculated from each window are extracted and combined in the feature vector. The extracted vectors are divided in two sets for training and testing set. 82 of 119 vector are used for training of neural network and 37 of 119 vectors for testing. The different window dimensions used in the experiments for detection process and different hidden neuron counts examined during the neural network training. The results obtained this experiments for different window dimensions and different hidden neurons are shown in Table 4.

Table 3. The experimental results of EWD method with different parameters of method and neural network classifier.

Window Dimension	ROC Analysis Results	K = 8				K = 16			
		Hidden Neuron				Hidden Neuron			
		10	20	30	40	10	20	30	40
30x30	Sensitivity (TPR)	0,88	0,88	0,75	0,75	0,88	0,75	0,75	0,75
	Fall-out(FPR)	0,48	0,28	0,41	0,38	0,38	0,34	0,28	0,34
40x40	Sensitivity (TPR)	0,75	0,75	0,75	0,75	0,88	0,75	0,88	0,75
	Fall-out(FPR)	0,45	0,45	0,38	0,07	0,48	0,34	0,31	0,24
50x50	Sensitivity (TPR)	0,88	0,75	0,75	0,75	0,88	0,88	0,75	0,75
	Fall-out(FPR)	0,38	0,34	0,28	0,34	0,48	0,28	0,41	0,38
60x60	Sensitivity (TPR)	0,75	0,75	0,75	0,88	0,75	0,75	0,88	0,75
	Fall-out(FPR)	0,41	0,41	0,45	0,34	0,41	0,24	0,48	0,24
70x70	Sensitivity (TPR)	0,75	0,75	0,75	0,75	0,75	0,75	0,75	0,75
	Fall-out(FPR)	0,28	0,41	0,21	0,38	0,48	0,45	0,41	0,34
80x80	Sensitivity (TPR)	0,75	0,75	0,75	0,75	0,75	0,75	0,75	0,75
	Fall-out(FPR)	0,48	0,45	0,31	0,41	0,41	0,48	0,48	0,41
		K = 32				K = 64			
		Hidden Neuron				Hidden Neuron			
		10	20	30	40	10	20	30	40
30x30	Sensitivity (TPR)	0,75	0,88	0,75	0,75	0,88	0,75	0,75	0,88
	Fall-out(FPR)	0,48	0,38	0,45	0,52	0,34	0,41	0,45	0,41
40x40	Sensitivity (TPR)	0,88	0,88	0,88	0,88	0,88	0,75	0,88	0,75
	Fall-out(FPR)	0,34	0,45	0,41	0,48	0,41	0,38	0,38	0,41
50x50	Sensitivity (TPR)	0,88	0,75	0,75	0,88	0,75	0,88	0,75	0,75
	Fall-out(FPR)	0,34	0,41	0,45	0,41	0,48	0,38	0,45	0,52
60x60	Sensitivity (TPR)	0,75	0,75	0,75	0,63	0,75	<b>1,00</b>	0,88	0,88
	Fall-out(FPR)	0,41	0,38	0,31	0,28	0,38	0,41	0,34	0,38
70x70	Sensitivity (TPR)	0,75	0,75	0,75	0,75	0,75	0,75	0,88	0,88
	Fall-out(FPR)	0,41	0,24	0,31	0,38	0,41	0,45	0,34	0,45
80x80	Sensitivity (TPR)	0,75	0,75	0,75	0,75	0,88	0,75	0,75	0,75
	Fall-out(FPR)	0,41	0,48	0,38	0,34	0,48	0,45	0,41	0,45
		All dataset: 119		Training Set: 82		Testing Set :37			

Table 4. The experimental results of multi-window statistical analysis for different window dimensions.

Window Dimension		Width of two window = 20				Width of two window = 30				Width of two window = 40			
		Hidden Neuron-				Hidden Neuron							
		10	20	30	40	10	20	30	40	10	20	30	40
30x30	Sensitivity (TPR)	0,75	0,88	<b>1,00</b>	0,88	0,875	0,875	0,875	0,875	0,875	0,875	0,75	0,75
	Fall-out(FPR)	0,14	0,21	0,21	0,21	0,207	0,172	0,172	0,138	0,276	0,241	0,207	0,345
40x40	Sensitivity (TPR)	0,88	1,00	0,88	<b>1,00</b>	<b>1,00</b>	0,875	0,875	0,875	0,875	0,75	0,75	<b>1,00</b>
	Fall-out(FPR)	0,28	0,21	0,45	0,172	0,379	0,276	0,207	0,379	0,138	0,172	0,172	0,172
50x50	Sensitivity (TPR)	0,88	0,88	0,75	0,75	0,875	0,75	0,75	0,75	0,75	0,75	0,75	0,75
	Fall-out(FPR)	0,38	0,17	0,21	0,21	0,138	0,172	0,138	0,172	0,138	0,207	0,138	0,138
60x60	Sensitivity (TPR)	<b>1,00</b>	0,75	0,75	0,63	0,75	<b>1,00</b>	0,875	0,75	<b>1,00</b>	0,875	0,75	0,75
	Fall-out(FPR)	0,34	0,17	0,31	0,34	0,207	0,379	0,448	0,31	0,276	0,379	0,345	0,172
70x70	Sensitivity (TPR)	0,75	0,75	0,75	0,75	0,75	0,75	0,75	0,75	0,75	0,75	0,75	0,75
	Fall-out(FPR)	0,28	0,21	0,24	0,21	0,138	0,207	0,241	0,138	0,345	0,345	0,448	0,172
80x80	Sensitivity (TPR)	0,75	0,75	0,75	0,75	0,75	0,875	0,75	0,625	0,75	0,875	0,625	0,75
	Fall-out(FPR)	0,45	0,31	0,31	0,28	0,276	0,483	0,379	0,345	0,31	0,414	0,138	0,345
		<b>All dataset:119</b>				<b>Training Set: 82</b>				<b>Testing Set :37</b>			

#### 4. Discussion

It is seen in Fig. 3 that the feature extraction methods have different sensitivity values after neural network classification process. The EWD method and newly used Multi-Window method is very good results for detection of microcalcification.

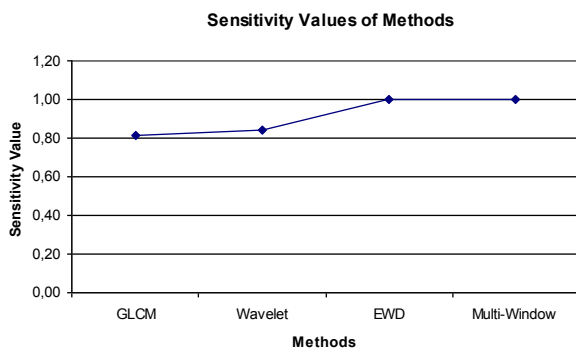


Fig. 3. Feature extraction methods and sensitivity values.

The testing process is implemented using MIAS database. The results of the study is seen in Table 5. And also our study is compared the other studies in the literature about microcalcification detection and sensitivity values of these studied are listed in Table 6.

A graphical user interface is developed in this study seen in Fig. 4. The trained and tested neural networks are saved and it was used in the interface. As you see in Fig. 2, the first stage is completed with training and testing of neural networks for each feature extraction method which has the best sensitivity value. In the graphical user interface, the mammogram image loaded first. After that the region of interest (ROI) is selected on the mammogram. One of the feature extraction method (neural network) is selected and applied on the ROI. As you see in the Fig. 4 step size and window size is utilized on the GUI and process is started after pressing the MCC Detection button. The microcalcification areas are highlighted on the image with surrounding squares.

Table 5. Comparison of feature extraction methods by using "Sensitivity" value.

Used Dataset	Feature Extraction Method Used	Sensitivity
MIAS dataset Training Set: 82 Testing Set :37 All Set:119	GLCM	0,81
	Wavelet Transform	0,84
	EWD	1,00
	Multi-Window	1,00

Table 6. Comparison of other studies about microcalcification detection.

Study	Used Dataset	Sensitivity
Rizzi [34]	MIAS and DDSM	0,98
L. Wei [33]	A special data set	0,98
I. El Naqa [31]	A special data set	0.94
P. Sajda [30]	A special data set	0.97
<b>Multi-window statistical analysis</b>	<b>MIAs</b>	<b>1,00</b>

## 5. Conclusion

There are very different and successful studies which have carried out in recent years in the field. In this study, it is focused detecting the MCs which are the early findings of the breast cancer. In this study it is proposed a new feature extraction method named multi-window statistical analysis and compared the well known methods in Table 5. The sensitivity values of similar studies in the literature are given in Table 6. The multi-window statistical analysis method is developed and used as a first time in this study.

It is applied on the two dimensional signals which are mammogram images in this study. And also a graphical user interface is developed. The developed user interface is also a framework for developing a computer aided detection system. Trained neural network could be entegrate to the this framewrok and GUI. In the future, changing the preprocessing step with different techniques of image processing and feature extraction will be studied in order to increase the sensitivity value of classification. New features will be added to the GUI.

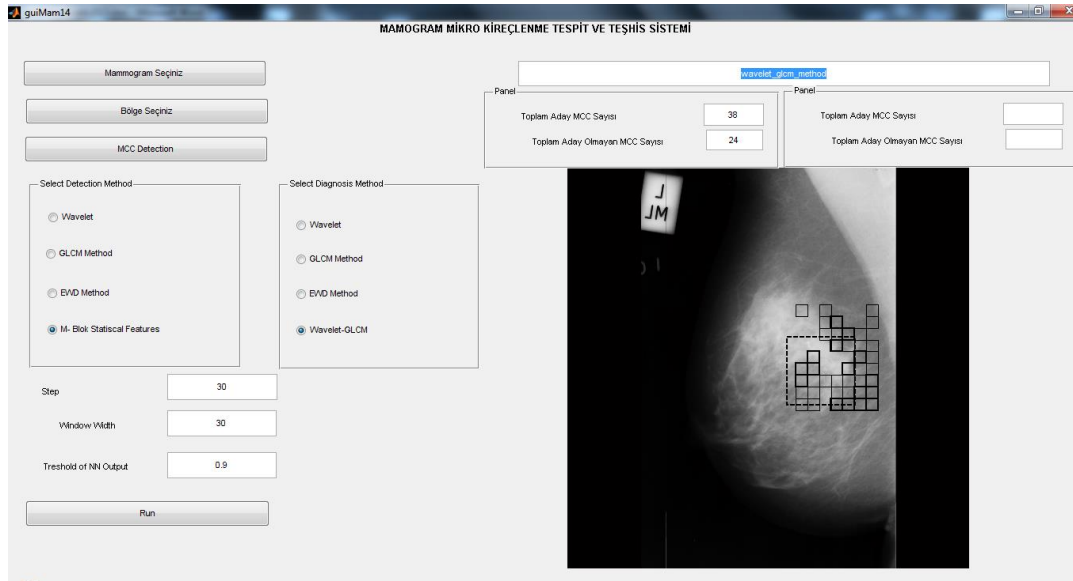


Fig. 4. Developed graphical user interface (GUI).

## References

- [1] M. Şengelen, T. Kutluk, D. Firat, Research and Control, (2007).
- [2] W. B. Lawrence, WB aunders, Philadelphia, PA, USA (1992).
- [3] G. Ertas, M. Sc. Thesis, Boğaziçi University, (2001).
- [4] M. Suganthi, M. Madheswaran, International Conference on Control, Automation, Communication and Energy Conservation, (2009), June 4-6, Perundurai, Tamilnadu.
- [5] B. Tuysuz, the MSc and PhD Thesis, Gaziantep University, (2007).
- [6] R. N. Strickland, H. Hahn, Journal of Trans. Med. Imag., **15**(2), 218 (1996).
- [7] D. B. Kopans, Breast Imaging, 3rd ed. Baltimore, MD: Williams & Wilkins, (2007).
- [8] H. D. Cheng, X. Cai, X. Chen, L. Hu, X. Lou, Pattern Recognition, **36**, 2967 (2003).
- [9] M. L. Giger, Comput. Sci. Eng., **2**, 39 (2000).
- [10] N. Karssemeijer, J. H. Hendriks, Eur. Radiol., **7**, 743 (1997).
- [11] L. Zhang, R. Sankar, W. Qian, Comput. Biol. Med., **32**, 515 (2002).
- [12] I. El Naqa, Y. Yang, Technology and Applications, **4**, 15 (2005).

- [13] R. M. Nishikawa, M. L. Giger, K. Doi, C. J. Vyborny, R. A. Schmidt, *Med. Biol. Eng. Comput.*, **33**, 174 (1995).
- [14] K. J. McLoughlin, P. J. Bones, N. Karssemeijer, *IEEE Trans. Med. Imag.*, **23**, 313 (2004).
- [15] W. Qian, F. Mao, X. Sun, Y. Zhang, D. Song, R. A. Clarke, *Comput. Med. Imag. Graph.*, **26**, 361 (2002).
- [16] M. N. Gurcan, Y. Assistant, A. E. Cetin, R. Ansari, *IEEE Signal Process. Lett.*, **4**, 213 (1997).
- [17] B. Caputo, E. L. Torre, S. Bouattour, G. E. Gigante, *Stud. Health Technol. Inf.*, **90**, 30 (2002).
- [18] P. Casaseca-de-la-Higuera, J. I. Arribas, E. Munoz-Moreno, C. Alberola-Lopez, in *Proc. 27th Annu. Int. Conf. Eng. Med. Biol. Soc.*, **1**, 49 (2005).
- [19] R. N. Strickland, H. Hahn, *IEEE Trans. Med. Imag.*, **15**, 218 (1996).
- [20] G. Lemaur, K. Drouiche, J. Deconinck, *IEEE Trans. Med. Imag.*, **22**, 393 (2003).
- [21] M. G. Mini, V. P. Devassia, T. Thomas, *J. Digit. Imag.*, **17**, 285 (2004).
- [22] R. Nakayama, Y. Uchiyama, K. Yamamoto, R. Watanabe, K. Namba, *IEEE Trans. Biomed. Eng.*, **53**, 273 (2006).
- [23] E. Regentova, L. Zhang, J. Zheng, G. Veni, *Med. Phys.*, **34**, 2206 (2007).
- [24] P. Yu, L. Guan, *IEEE Trans. Med. Imag.*, **19**, 115 (2000).
- [25] J. Jiang, B. Yao, A. M. Wason, *Comput. Med. Imag. Graph.*, **31**, 49 (2007).
- [26] Y. Peng, B. Yao, J. Jiang, *Artif. Intell. Med.*, **37**(1), 43 (2006).
- [27] L. Bocchi, G. Coppini, J. Nori, G. Valli, *Med. Eng. Phys.*, **26**, 303 (2004).
- [28] M. N. Gurcan, H. P. Chan, B. Sahiner, L. Hadjiiski, N. Petrick, M. A. Helvie, *Acad. Radiol.*, **9**, 420 (2002).
- [29] A. Papadopoulos, D. I. Fotiadis, A. Likas, *Artif. Intell. Med.*, **25**, 149 (2002).
- [30] P. Sajda, C. Spence, J. Pearson, *IEEE Trans. Med. Imag.*, **21**, 239 (2002).
- [31] I. El Naqa, Y. Yang, M. N. Wernick, N. P. Galatsanos, R. M. Nishikawa, *IEEE Trans. Med. Imag.*, **21**, 1552 (2002).
- [32] P. Singh, V. Kumar, H. K. Verma, D. Singh, in *Proc. 28th Annu. Int. Conf. Eng. Med. Biol. Soc.*, **1**, 4747 (2006).
- [33] L. Wei, Y. Yang, R. M. Nishikawa, M. N. Wernick, A. Edwards, *IEEE Trans. Med. Imag.*, **24**, 1278 (2005).
- [34] M. Rizzi, M. D'Aloia, C. Guaragnella, B. Castagnolo, *IEEE Transactions on Man and Cybernetics, Part A: Systems and Humans*, **42**, 1385 (2012).
- [35] R. Peng, P. K. HaoChenVarshney, *IEEE Journal of Selected Topics in Signal Processing*, **3**, 62 (2009).
- [36] U. Orhan, M. Physician, M. Ozer, 15th National Biomedical Engineering Meeting (BIYOMUT), (2010).
- [37] Pham, L. Dzung, Xu, Chenyang, Prince, L. Jerry, *Annual Review of Biomedical Engineering*, **2**, 315 (2000).
- [38] Linda G. Shapiro, George C. Stockman, *Computer Vision*, 279-325, Prentice-Hall, New Jersey (2001).
- [39] N. Otsu, *IEEE Trans. Sys., Man., Cyber.*, **9**, 62 (1979).
- [40] E. Arias-Castro, D. L. Donoho, *Annals of Statistics*, **37**, 1079 (2009).
- [41] G. R. Arce, *Nonlinear Signal Processing: A Statistical Approach*, Wiley, New Jersey, USA, (2005).
- [42] R. M. Haralick, K. Shanmugam, *IEEE Transactions on Systems, Man, and Cybernetics*, **6**, 610 (1973)
- [43] A. Grossmann, J. Morlet, *SIAM Journal on Mathematical Analysis*, **15**, 723 (1984).
- [44] U. Orhan, M. Hekim, Mahmut Ozer, *Journal of the Faculty of Engineering and Architecture of Gazi University*, **26**, 575 (2011).
- [44] Michael Heath, Kevin Bowyer, Daniel Kopans, Richard Moore, W. Philip Kegelmeyer, in *Proceedings of the Fifth International Workshop on Digital Mammography*, M. J. Yaffe, ed., 212-218, Medical Physics Publishing, 2001
- [45] Michael Heath, Kevin Bowyer, Daniel Kopans, W. Philip Kegelmeyer, Richard Moore, Kyong Chang, S. MunishKumaran, in *Digital Mammography*, 457-460, Kluwer Academic Publishers, 1998; *Proceedings of the Fourth International Workshop on Digital Mammography*.

---

\*Corresponding author: iseriismail@gmail.com